

STRAIN RATE EFFECT ON LONG-TERM CONSOLIDATION OF OSAKA BAY CLAY

YOICHI WATABEⁱ⁾, KAORU UDAKAⁱⁱ⁾ and YOSHIYUKI MORIKAWAⁱⁱⁱ⁾

ABSTRACT

The consolidation characteristics of clay, based on the isotache concept in which the strain rate effect is considered, have been studied by many researchers. Most of these studies are aimed at calculating the secondary consolidation with high accuracy in order to evaluate the long-term settlement of large structures. In this study, as the first step toward improving the accuracy of the evaluation of long-term settlement at the Kansai International Airport, the consolidation characteristics of Osaka Bay clay are examined and organized based on the isotache concept. This study proposes a simplified model based on the isotache concept by using a compression curve and the relationship between the consolidation yield stress and the strain rate. The former and the latter are obtained from the constant rate of strain consolidation (CRS) tests and long term consolidation (LT) tests, respectively. The latter is expressed by an equation with three isotache parameters. This model is very practical because it requires a minimum of only one CRS test and one LT test. It is widely applicable to the Osaka Bay clay. The isotache parameters used in this model can be commonly determined for the Osaka Bay clays retrieved from various depths at the Kansai International Airport.

Key words: clay, isotache, long-term consolidation, secondary consolidation, strain rate (IGC: D5)

INTRODUCTION

The Kansai International Airport, located offshore of Senshu in Osaka Bay, is characterized as an area with a large water depth and very thick clay deposits. The settlement of the shallow and soft Holocene clay deposits can be controlled by ground improvement such as sand drains. However, the residual settlement that occurred after the inauguration of the airport mainly in the deep and stiff Pleistocene clay deposit cannot be controlled because ground systems cannot be improved for larger depths. Therefore, the evaluation of the settlement is very important.

The first phase of the Kansai International Airport Project, which was inaugurated in September 1994, is a large man-made island of approximately 510 ha located 5 km from Senshu in Osaka Bay. The average water depth was 18 m, and the incremental consolidation pressure reached 450 kPa with reclamation. The second phase of the airport has also been constructed as a man-made island of approximately 545 ha (Photo 1). The second phase with a parallel runway has been operational since August 2007. The average water depth was 19.5 m and thick clay layers up to 400 m in depth alternated with some sandy layers. The incremental consolidation pressure reached 600 kPa with reclamation.

Because airport facilities are generally characterized by



Photo 1. An aerial photograph of the Kansai International Airport taken in March 2007

their flatness, long-term settlement is ranked as one of the most important issues in their management. A one-dimensional elastoplastic consolidation analysis has been carried out to evaluate the consolidation settlement of the Kansai International Airport by using a compiled geo-information database. The long-term consolidation settlement has been calculated using the coefficient of secondary consolidation C_α corresponding to the consolidation yield stress.

In recent years, researchers have focused on the

ⁱ⁾ Leader, Soil Mechanics and Geo-environment Research Group, Port and Airport Research Institute, Japan (watabe@ipc.pari.go.jp).

ⁱⁱ⁾ Tokyo Geotechnical Center, OYO Corporation, Japan.

ⁱⁱⁱ⁾ Leader, Soil Stabilization Research Group, Port and Airport Research Institute, Japan (formerly Kansai International Airport Co., Ltd.). The manuscript for this paper was received for review on August 6, 2007; approved on April 8, 2008.

Written discussions on this paper should be submitted before March 1, 2009 to the Japanese Geotechnical Society, 4-38-2, Sengoku, Bunkyo-ku, Tokyo 112-0011, Japan. Upon request the closing date may be extended one month.

isotache concept in which the effect of the strain rate on the compression characteristics is considered because the secondary consolidation has to be calculated with high accuracy in order to evaluate the long-term settlement (e.g., Leroueil et al., 1985; Yin et al., 1994; Adachi et al., 1996; Kim and Leroueil, 2001; Imai et al., 2005; Tanaka et al., 2006). In this study, as the first step for the researchers toward improving the accuracy in evaluating the long-term consolidation settlement, the consolidation characteristics of the Osaka Bay clay will be discussed and organized based on the isotache concept.

The characteristics of the Osaka Bay clay collected from the site of the Kansai International Airport have been widely studied. In the investigation of the seabed soil at the site, undisturbed clay samplings were analyzed by using a hydraulic-operated thin-walled tube sampler with a fixed piston for soft clays or a rotary-type double-tube sampler for stiff clays. A wire-line method was used for efficient sampling (Kanda et al., 1991; Horie et al., 1984). Watabe and Tsuchida (2001) confirmed that the sample quality was classified as excellent, with very little disturbance. Tanaka et al. (2003) obtained a continuous depth profile for the piezocone test (CPTU) tip resistance at large depths and indicated that the clay deposit was significantly heterogeneous. On the other hand, Watabe et al. (2007a) carried out laboratory physical tests and a constant rate of strain consolidation (CRS) tests for specimens trimmed to 25-mm intervals from a one-meter-long undisturbed sample. Because the coefficients of variation COV for all the examined soil parameters were smaller than 0.1, they concluded that the clay layer was a homogeneous deposit in which each specimen trimmed from the one-meter-long sample can be considered to be its representative sample. Tanaka and Locat (1999) indicated that the clay fabric was characterized by abundant diatomaceous microfossils, which are closely related to the mechanical properties. The K_0 -consolidation (Watabe et al., 2003) and undrained shear strength (Watabe and Tsuchida, 2001; Watabe et al., 2002) were also studied. The consolidation settlement of the airport was discussed by many researchers (e.g., Nakase, 1987; Duncan, 1993; Akai, 2000; Mimura and Jang, 2005). Recently, Kobayashi et al. (2005) developed a new reasonable analysis method in which they coupled the one-dimensional vertical consolidation for the clay layers and the two-dimensional seepage for the sand layers.

There are three main approaches for both the practical and theoretical evaluations of the consolidation settlement, and these can be listed as follows:

- (i) The coupling of Terzaghi's one-dimensional consolidation theory and the constant C_α concept.
- (ii) The end of primary consolidation (EOP) concept (Mesri and Choi, 1985) and the constant C_α/C_c concept (Mesri and Castro, 1987).
- (iii) The isotache concept (Šuklje, 1957)

Here, $C_{\alpha\epsilon}$ denotes the coefficient of secondary consolidation in strain. In practice, approach (i) is the most widely used. After EOP, the incremental strain caused by secondary consolidation varies linearly against the

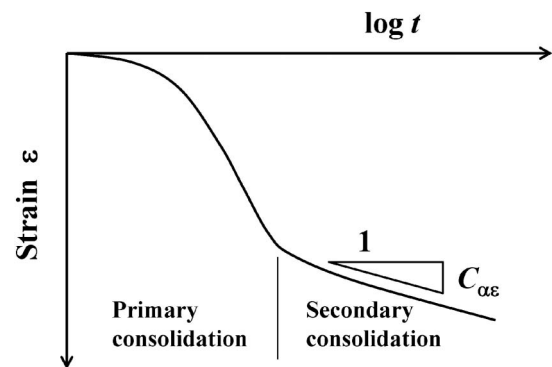


Fig. 1. Consolidation curve (ϵ - $\log t$ curve) indicating primary consolidation and secondary consolidation

logarithmic elapsed time after loading, $\log t$. The incremental strain corresponding to one cycle of logarithmic time during the secondary consolidation is denoted as $C_{\alpha\epsilon}$ as shown in Fig. 1. The secondary consolidation is calculated by assuming that $C_{\alpha\epsilon}$ is a constant value. The long-term settlement of the Kansai International Airport has been evaluated using approach (i) with a constant value of $C_{\alpha\epsilon}$.

Approach (ii) is a clear-cut concept, which is applicable in practice. From the EOP compression curves, Mesri and Choi (1985) empirically determined that the consolidation yield stresses obtained in the laboratory and the field are equivalent. The constant C_α/C_c concept proposed by Mesri and Castro (1987) is useful to explain the secondary consolidation with regard to the delayed creep consolidation (Bjerrum, 1967) in which the ϵ - $\log p$ curve shifts downward with time. Because time is introduced explicitly as “elapsed time” rather than being implicitly denoted as “strain rate,” this approach is essentially the same as approach (i). The constant C_α/C_c concept is consistent with the isotache concept; however, its application is limited because secondary consolidation continues infinitely against logarithmic time, i.e., the strain increases to infinity at infinite time. However, Leroueil (2006) denied the generality of the EOP concept based on his experience in which the consolidation yield stress corresponding to the EOP compression curve obtained in the laboratory is significantly larger than that observed in the field.

Approach (iii) is a concept proposed by Šuklje (1957), which involves viscosity and introduces a unique relationship between the strain and the consolidation pressure corresponding to the strain rate. This concept, which focuses on the strain rate effect, has attracted a lot of attention in recent researches on consolidation. The isotache concept was proposed more than 50 years ago; however, it continues to be studied in academia. There have been many studies on the long-term consolidation with regard to viscosity (e.g., Leroueil et al., 1985; Yin et al., 1994; Adachi et al., 1996; Kim and Leroueil, 2001). Imai et al. (2005) and Tanaka et al. (2006) clarified that the isotache concept is applicable to the long-term consolidation of the Osaka Bay clay.

In this paper, we propose a simplified model of the isotache concept and apply it to the long-term consolidation of Osaka Bay clay; we then tabulate the isotache parameters introduced in the model. We also discuss the applicability of the constant C_a/C_c concept in association with the isotache concept. However, we will not discuss the scale effect of the thickness of the specimen on the consolidation that is closely related to the EOP concept.

SIMPLIFIED MODEL OF THE ISOTACHE CONCEPT

Basic Concept

In this paper, in order to model the isotache concept, we use very simple equations proposed by Leroueil et al. (1985). These are expressed by Eqs. (1) and (2).

$$\frac{p'}{p'_c} = f(\varepsilon) \quad (1)$$

$$p'_c = g(\dot{\varepsilon}) \quad (2)$$

Here, $\dot{\varepsilon}$ is the strain rate defined as $d\varepsilon/dt$.

The isotache concept is only applicable to visco-plastic deformation, which is the elastic deformation deducted from the total deformation. For clarity, we employ the ε_{vp} -log p' relationship, where ε_{vp} is the visco-plastic strain, which is defined as the difference between the total strain ε obtained from the consolidation test and the elastic strain ε_e . We then use Eqs. (3), (4) and (5).

$$\varepsilon_{vp} = \varepsilon - \varepsilon_e \quad (3)$$

$$\frac{p'}{p'_c} = f(\varepsilon_{vp}) \quad (4)$$

$$p'_c = g(\dot{\varepsilon}_{vp}) \quad (5)$$

In order to obtain the relationships expressed by the above equations such as Eqs. (4) and (5), the CRS and LT tests are required to be performed, respectively. The de-

tails will be described later.

The parameter ε_e is defined as the strain expressed by the straight line passing through the points $(p', \varepsilon) = (1 \text{ kPa}, 0)$ and $(\sigma'_{v0}, \varepsilon_0)$ on the ε -log p' curve. The value that corresponds to the effective consolidation pressure p' is denoted as $\varepsilon_e(p')$. The slope of the straight line is denoted as C_{se} . Here, σ'_{v0} denotes the overburden effective stress and ε_0 denotes the strain at $p' = \sigma'_{v0}$. C_{se} denotes the swelling index in strain. From the ε -log p' curve obtained from the CRS test, ε_{vp} is calculated as the difference between ε and ε_e ; the ε_{vp} -log p' curve is then obtained. These procedures are illustrated in Fig. 2(a). The parameter p' is normalized by the value of the consolidation yield stress p'_c read from the ε_{vp} -log p' curve, and subsequently the ε_{vp} -log p'/p'_c curve that corresponds to Eq. (4) is obtained. Hereafter, this curve is called as the “reference compression curve” (Fig. 2(b)). The ε_{vp} -log p' curve that corresponds to a certain visco-plastic strain rate $\dot{\varepsilon}_{vp}$ is obtained by multiplying p'/p'_c of the reference compression curve with $p'_c(\dot{\varepsilon}_{vp})$.

Because the pore water pressure u is not measured in the LT test, the effective consolidation pressure p' cannot be evaluated. However, when we consider the secondary consolidation stage, we can assume that the excess pore water pressure is essentially zero ($\Delta u = 0$), i.e., p' is equivalent to p . Therefore, $\dot{\varepsilon}$ essentially coincides with $\dot{\varepsilon}_{vp}$. Hereafter, in order to avoid confusion, we use $\dot{\varepsilon}_{vp}$ and p' instead of $\dot{\varepsilon}$ and p , respectively, when Δu is essentially zero.

The parameter $\dot{\varepsilon}_{vp}$ is calculated from the secondary consolidation section of the ε -log t curve (consolidation curve) observed in the LT test under a consolidation pressure of p' ; $\dot{\varepsilon}_{vp}$ is then obtained as a function of p' and $\dot{\varepsilon}_{vp}$. The quantity p'/p'_c is obtained as a function of ε_{vp} from the reference compression curve for some (p', ε_{vp}) data corresponding to $\dot{\varepsilon}_{vp}$; p'_c is then calculated from p'/p'_c and p' . This procedure is repeated for some $\dot{\varepsilon}_{vp}$ values, and then the $(p'_c, \dot{\varepsilon}_{vp})$ data are obtained. The above procedures are according to the real data treatment, which is de-

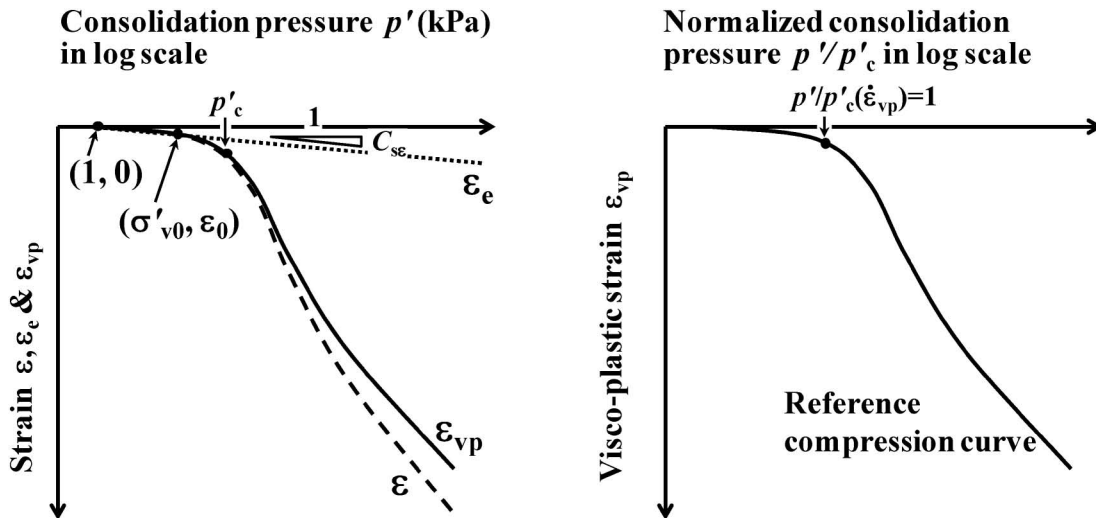


Fig. 2. Compression curve (ε -log p' curve): (a) definition of ε_e and ε_{vp} and (b) reference compression curve

scribed later. Essentially, from the LT test, we can obtain the ε_{vp} - $\log p'$ relationship as a function of $\dot{\varepsilon}_{vp}$.

In some cases, we could not obtain good agreement between the reference compression curve from the CRS test and the (p', ε_{vp}) values corresponding to $\dot{\varepsilon}_{vp}$ from the LT test. Despite our attempts to select specimens from the nearest depths for both the LT and CRS tests, the properties, representing the level of developed structure, of the real specimens were slightly different, such as grain size distribution, the natural water content w_n , the consolidation yield stress p'_c , the shape of the reference compression curve, because they were retrieved from a natural deposit. Therefore, in such cases, we attempted to obtain good agreement between them by the expansion or contraction of the reference compression curve in the ε_{vp} direction.

Model Equation of the Isotache Concept

Hereafter, we will try to express the p'_c - $\dot{\varepsilon}_{vp}$ relationship in Eq. (5) as a mathematical model. The isotache concept will be summarized below after reviewing the existing knowledge.

Leroueil (2006) emphasized that the slope α which is defined as $\Delta \log p'_c / \Delta \log \dot{\varepsilon}_{vp}$, decreases when $\dot{\varepsilon}_{vp}$ decreases to a very small value; this statement was based not only on the result of his study of Eastern Canada clay but also the data on the Osaka Bay clay mentioned in Imai et al. (2005).

Tanaka (2005) discussed the LT test results based on a linear p'_c - $\log \dot{\varepsilon}_{vp}$ relationship. In this case, despite the introduction of the isotache concept, the long-term consolidation is unrealistically described because p'_c decreases to zero with $\dot{\varepsilon}_{vp}$, thus implying that consolidation settlement does not converge against logarithmic time.

Ohmukai and Imai (2006) modeled the isotache concept in a manner such that the slope α becomes smaller when $\dot{\varepsilon}_{vp}$ decreases. They noted that the value of $p'_c(\dot{\varepsilon}_{vp})$ becomes constant when $\dot{\varepsilon}_{vp}$ decreases to values smaller than $1.0 \times 10^{-11} \text{ s}^{-1}$. They set the lower limit of p'_c at a very small $\dot{\varepsilon}_{vp}$ as $0.71 \times p'_{c0}$ for the Osaka Bay clay by using the relaxation test proposed by Yoshikuni et al. (1994). Here, p'_{c0} is the value of p'_c at $\dot{\varepsilon}_{vp} = 3.3 \times 10^{-6} \text{ s}^{-1}$. In this case, a certain $\dot{\varepsilon}_{vp}$ smaller than $1.0 \times 10^{-11} \text{ s}^{-1}$ gives a p'_c value representing the lower limit of the ε_{vp} - $\log p'$ curve; however, the lower limit of p'_c gives innumerable $\dot{\varepsilon}_{vp}$ values in a range smaller than $1.0 \times 10^{-11} \text{ s}^{-1}$. This implies that the relationship between $\dot{\varepsilon}_{vp}$ and p'_c is not one-on-one. In this regard, their model has a drawback with regard to the long-term settlement calculation.

Kobayashi et al. (2005) have proposed model equations, as shown in the following two expressions, in which $\alpha = \Delta \log p'_c / \Delta \log \dot{\varepsilon}_{vp}$ decreases with $\dot{\varepsilon}_{vp}$. The first expression is expressed by Eq. (6):

$$\ln p'_c = a_1 + a_2 \ln \dot{\varepsilon}_{vp} \quad (6)$$

Here, a_1 and a_2 are constants. Because the $\log p'_c$ - $\log \dot{\varepsilon}_{vp}$ relationship is linear in Eq. (6), the model is unrealistic as p'_c becomes zero when $\dot{\varepsilon}_{vp}$ decreases to zero. However, Eq. (6) has a slight advantage with regard to a linear $\log p'_c$

- $\log \dot{\varepsilon}_{vp}$ relationship rather than a linear p'_c - $\log \dot{\varepsilon}_{vp}$ relationship, because p'_c in the former gently decreases, but larger than zero, with decreasing $\dot{\varepsilon}_{vp}$. The second expression is given by Eq. (7):

$$p'_c = p'_{cL} + b_1 \exp(b_2 \ln \dot{\varepsilon}_{vp}) \quad (7)$$

Here, b_1 and b_2 are constants and p'_{cL} is the lower limit of p'_c . When $\dot{\varepsilon}_{vp}$ decreases to zero in Eq. (7), p'_c converges to p'_{cL} . In this paper, we revise Eq. (7) to yield as Eq. (8):

$$\ln \frac{p'_c - p'_{cL}}{p'_{cL}} = c_1 + c_2 \ln \dot{\varepsilon}_{vp} \quad (8)$$

Here, c_1 and c_2 are constants. Eq. (8) is a dimensionless expression; however, it is equivalent to Eq. (9) in a dimensional form.

$$\ln(p'_c - p'_{cL}) = c'_1 + c'_2 \ln \dot{\varepsilon}_{vp} \quad (9)$$

Here, c'_1 and c'_2 are constants, and c'_1 and p'_{cL} are inter-related by Eq. (10):

$$c'_1 = c_1 + \ln p'_{cL} \quad (10)$$

Equation (8) is apparently complicated because c_1 increases to infinity when p'_{cL} decreases to zero. However, we can derive Eq. (6) from Eq. (9) when p'_{cL} decreases to zero.

The parameters c_1 and c'_1 are equal to $\ln \{(p'_c - p'_{cL}) / p'_{cL}\}$ and $\ln(p'_c - p'_{cL})$, respectively, at $\dot{\varepsilon}_{vp} = 1$, i.e., they represent the relative position of the $\log p'_c$ - $\log \dot{\varepsilon}_{vp}$ curve. The parameters c_2 and c'_2 ($c_2 = c'_2$) represent the level of strain rate dependency expressed by the slope in $\log(p'_c - p'_{cL})$ - $\log \dot{\varepsilon}_{vp}$ diagram. The compressibility which reflects the level of developed skeletal structure is represented by the reference compression curve expressed by Eq. (4). Consequently the reference compression curve and three isotache parameters (c_1 , c_2 and p'_{cL}) are required in the proposed isotache model.

The isotache model is derived through observation of visco-plastic contraction behavior in a soil element, excess pore pressure dissipation which is governed by the coefficient of consolidation c_v and the thickness of soil layer is not directly considered. The settlement can be calculated by applying the differential method on incremental time Δt with the reference compression curve (Eq. (4)) and strain rate effect (Eq. (8)), when we have separately obtained the excess pore pressure dissipation; i.e., temporal variation of effective consolidation pressure (p' - t relationship). For more accurate calculation, coupled analysis between soil skeletal contraction and drainage is required.

CLAY SAMPLES

The clay samples for the CRS and LT tests were Osaka Bay marine clays retrieved from geotechnical investigation sites of the second-phase project of the Kansai International Airport. Approximately 20 m of the thick surface layer was composed of Holocene clay deposits called Ma13. Below this layer was a very thick layer of Pleistocene deposits that comprised alternating clay and sand

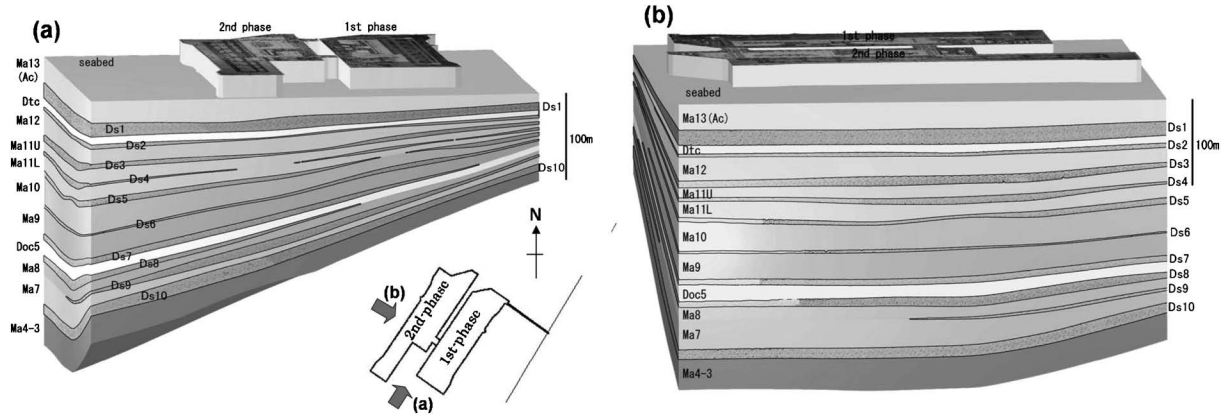


Fig. 3. Stratigraphic model at the Kansai International Airport: (a) cross-shore direction and (b) along-shore direction

Table 1. Physical properties of the clay samples

Layer	Ma13	Ma12	Ma11	Ma10	Ma9	Ma8	Ma7	Ma4	Ma13Re
Undisturbed	Yes	Yes	Yes	Yes	Yes	Yes	Yes	Yes	No
Reconstituted	No	No	No	No	No	No	No	No	Yes
Depth (C.D.L. – m)	39	61	109	142	167	208	223	264	30–40
Overburden effective stress σ'_{v0} (kPa)	88	286	619	857	1030	1348	1457	1802	(98)
Consolidation yield stress p'_c (kPa)	122	439	737	1294	1403	1698	1887	2512	134
Overconsolidation ratio OCR	1.39	1.53	1.19	1.51	1.36	1.26	1.30	1.39	(1.37)
Soil particle density ρ_s (g/cm ³)	2.66	2.66	2.67	2.69	2.70	2.72	2.70	2.67	2.70
Liquid limit w_L (%)	75.1	102.6	88.9	84.2	98.3	91.8	100.4	93.6	91.3
Plastic limit w_P (%)	31.9	40.8	34.4	36.4	37.4	35.8	37.8	35.3	30.3
Plasticity index I_p	43.2	61.8	54.5	47.8	60.9	56.0	62.6	58.3	61.0
Natural water content w_n (%)	62.0	83.8	55.4	48.6	54.0	49.9	49.0	50.6	71.5

layers. Clay layers are classified into marine and non-marine layers. Marine clays are numbered starting from Ma13 and the numbering decreases with depth. The sand layers are numbered starting from Ds1, which is deposited just below Ma13, and the numbering increases with depth. Layers Ma6 and Ma5 were missing due to degradation. Non-marine clays deposited between Ds1 and Ds2 are named as Dtc, and those deposited between Ds7 and Ds8 are named as Doc5.

In this study, undisturbed marine clay samples of Ma13, Ma12, Ma11, Ma10, Ma9, Ma8, Ma7, and Ma4 are considered. A stratigraphic model of the site is illustrated in Fig. 3. The reconstituted Ma13, which was remolded and preliminarily consolidated under 98 kPa and named as Ma13Re, was also tested. The retrieval depth, overburden effective stress σ'_{v0} , and representative values of the physical properties of the clay samples are listed in Table 1. Note that the soil properties for each specimen examined in this study were slightly different from the representative values because natural clay deposits are not perfectly homogeneous.

LABORATORY TESTS

In order to obtain the data sets required for Eqs. (3), (4), and (5), a series of CRS and LT tests were conducted.

CRS Test

CRS tests were conducted following JIS A 1227. A trimmed clay sample with a diameter of 60 mm and a height of approximately 25 mm was inserted into a stainless consolidation ring with an inner diameter of 60 mm and a height of 20 mm; subsequently, both the ends were trimmed off. A consolidation cell was assembled for the CRS test, and it was set up on a loading table. The cell was filled with de-aired water; a hydraulic pressure of 98 kPa was applied as backpressure while the piston uplift was prevented by the loading frame. A hydraulic pressure transducer (capacity of 3500 kPa and accuracy of 0.88 kPa (capacity of 700 kPa and accuracy of 0.18 kPa for Ma13)) was installed on the bottom metal plate of the consolidation cell by using a porous metal with a diameter of 10 mm. The vertical axial load was measured by a load cell (capacity of 49 kN and accuracy of 0.012

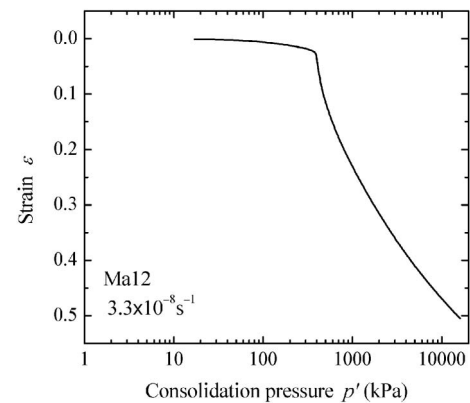
Table 2. Loading stages for LT tests

Sample	Pressures for preliminary consolidation (kPa)		Pressures for long term consolidation (kPa)
	24 hours incremental loading	7 days loading at σ'_{v0}	
Ma13	10→29→	88→	98, 137, 206, 235, 353 and 412
Ma12	39→79→157→	294→	333, 373, 412, 451, 490, 529, 608, 686, 882 and 1370
Ma11	39 (2 hours)→	628 (24 hours)→	647, 667, 686, 706, 726, 745, 1000 and 1569
Ma10	39 (2 hours)→	863 (24 hours)→	922, 891, 1040, 1118, 1196, 1236, 1275 and 1667
Ma9	39 (2 hours)→	1059 (24 hours)→	1138, 1177, 1216, 1255, 1314, 1393, 1471 and 2059
Ma8	39 (2 hours)→	1373 (24 hours)→	1412, 1471, 1530, 1589, 1648, 1726, 1785 and 2040
Ma7	39 (2 hours)→	1491 (24 hours)→	1549, 1608, 1667, 1726, 1785, 1844, 1922 and 2177
Ma4	39 (2 hours)→	1863 (24 hours)→	1902, 1961, 2059, 2157, 2256, 2354, 2452 and 3138
Ma13Re	10→29→	88→	118, 137, 206, 275, 343 and 412

kN (capacity of 19.6 kN and accuracy of 0.0049 kN for Ma13)) that was installed between the piston and the loading frame. The measured load was corrected for the uplift force caused by the backpressure. The specimen was contracted at a constant $\dot{\epsilon}$ of 0.02%/min ($= 3.3 \times 10^{-6} \text{ s}^{-1}$). However, in the case of Ma12, an $\dot{\epsilon}$ value of 0.0002%/min ($= 3.3 \times 10^{-8} \text{ s}^{-1}$) was preferred to obtain a compression curve with significant yielding. The settlement was measured by a linear gauge (capacity of 20 mm and accuracy of 0.001 mm (capacity of 10 mm and accuracy of 0.0001 mm for tests with an $\dot{\epsilon}$ of $3.3 \times 10^{-8} \text{ s}^{-1}$)).

Long Term Consolidation Test (LT test)

Similar to the CRS test, an oedometer was assembled with a specimen with a diameter of 60 mm and a height of 20 mm and it was installed into a stainless consolidation ring. In order to prepare drainage interfaces, a porous metal plate was installed on the bottom plate and the top piston. The load for consolidation was applied through a lever system by counter weights. The settlement was measured by a linear gauge (capacity of 20 mm and accuracy of 0.001 mm). The test conditions are listed in Table 2. In Ma13, Ma12, and Ma13Re, the preliminary consolidation pressures applied were incremented every 24 h in a ratio $\Delta p/p$ ranging from 1.0 to 2.0; subsequently, a consolidation pressure equivalent to the value of σ'_{v0} was applied for seven days. Here, Δp denotes the incremental consolidation pressure and p denotes the consolidation pressure in the previous stage. In order to prevent the specimen from swelling, the specimens were not submerged before yielding but allowed to remain wet. In other tests (Ma11, Ma10, Ma9, Ma8, Ma7, and Ma4), a consolidation pressure of 39 kPa was applied for 2 hours to prevent swelling, and then a consolidation pressure equivalent to σ'_{v0} was applied for 24 hours. Subsequently, a target pressure was applied for the long term consolidation until $\dot{\epsilon}$ decreased to $3.3 \times 10^{-9} \text{ s}^{-1}$. Six to ten target pressures in the range of σ'_{v0} to $2.0 \times p'_c$ were specified for each sample, as listed in Table 2.

**Fig. 4.** Compression curve (ϵ -log p' curve) for Ma12

TEST RESULTS

CRS Test

As an example of the compression curves obtained by the CRS tests, the ϵ -log p' curve for Ma12 is shown in Fig. 4. From the figure, the consolidation yield stress is determined to be 439 kPa. Because σ'_{v0} was 286 kPa, the overconsolidation ratio OCR ($= p'_c/\sigma'_{v0}$) is calculated as 1.5. This value is consistent with the fact that the OCR of the marine clay deposit around the Kansai International Airport is in the range of 1.3 to 1.5 (Horie et al., 1984; Kanda et al., 1991; Watabe et al., 2003). The compression curve is characterized by an overshooting pattern around p'_c . This pattern is typically observed for structured clays. We will plot this compression curve based on the method illustrated in Fig. 2. The parameter ϵ_{vp} is calculated as the difference between the observed strain ϵ and ϵ_c . The parameter p' is normalized by p'_c , and subsequently the reference compression curve (ϵ_{vp} -log p'/p'_c curve corresponding to Eq. (4)) is obtained. The reference compression curves for all the examined samples are shown in Fig. 5.

The curve for Ma13Re shows a bi-linear relationship pattern, which buckles at p'_c . This pattern is typically observed for non-structured clays. The Ma13 curve is also

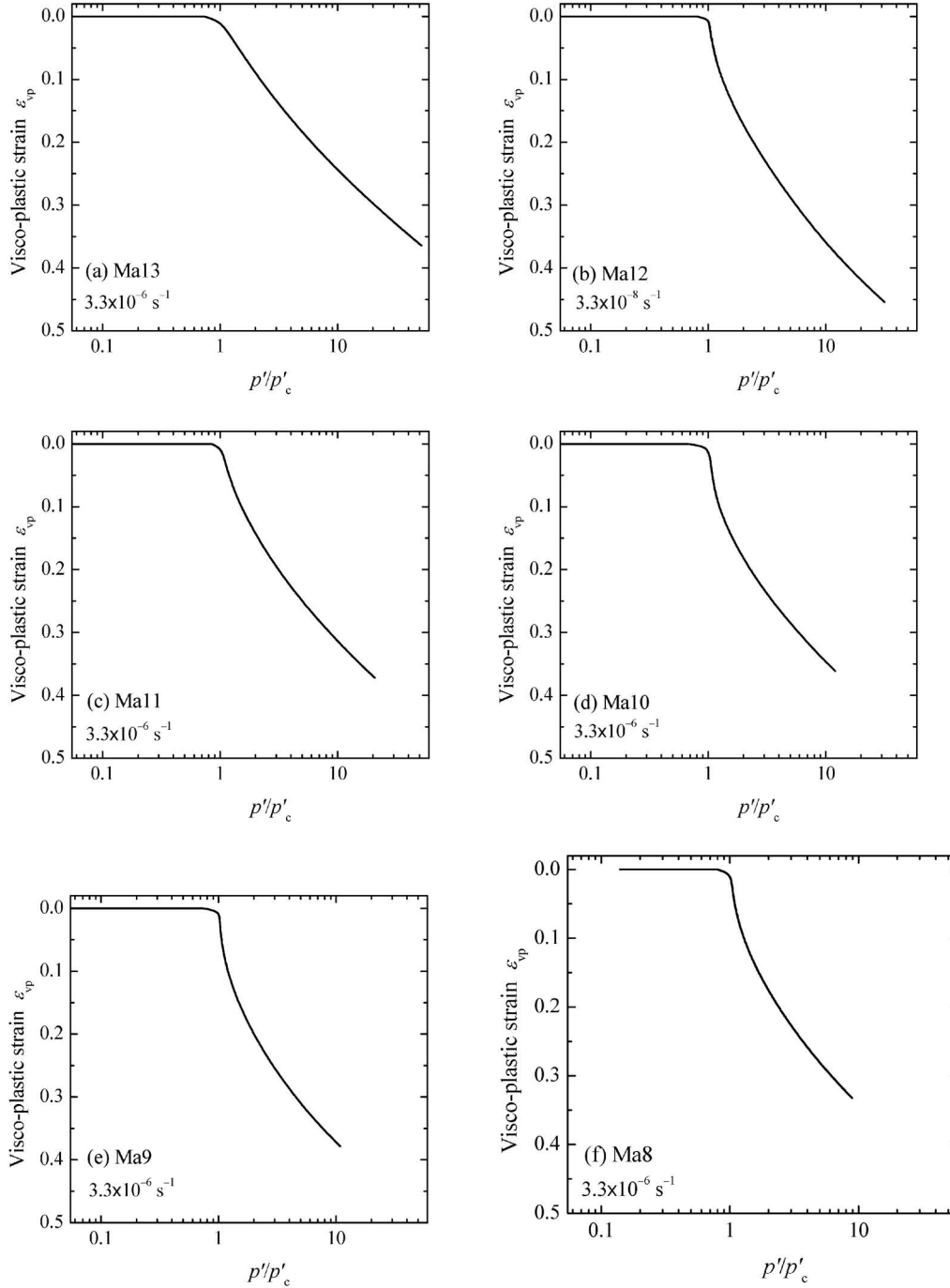


Fig. 5. Reference compression curves (ε_{vp} - $\log p'/p'_c$ curves): (a) Ma13, (b) Ma12, (c) Ma11, (d) Ma10, (e) Ma9, (f) Ma8, (g) Ma7, (h) Ma4 and (i) Ma13Re

similar to this. A unique reference curve is formed by the Ma12 to Ma4 curves, and it exhibits overshooting at around p'_c and a concave shape in the normal consolidation range. This tendency is the most significant in Ma12. These descriptions are clearly illustrated in Fig. 6 in which all the reference compression curves are superimposed.

LT Test

The consolidation curves (ε - $\log t$ curves) obtained from the LT tests are shown in Fig. 7. The parameter ε was calculated using the initial specimen height ($= 20$ mm) and it

was offset by the strain after seven days of preliminary consolidation under σ'_{v0} . Thus, all the consolidation curves start from zero strain.

In a normal consolidation range in which long-term p is greater than p'_c , secondary consolidation appears after the EOP. The curves in the secondary consolidation stage are concave shaped, indicating that the slope $\Delta\varepsilon_{vp}/\Delta \log t$ gradually decreases with the logarithmic time. In Ma13 to Ma10 and Ma13Re, the EOP appears after the inflection point between the convex curve and the concave curve; however, in Ma9 to Ma4, the EOP appears on the convex curve before the inflection point. The latter phenomenon

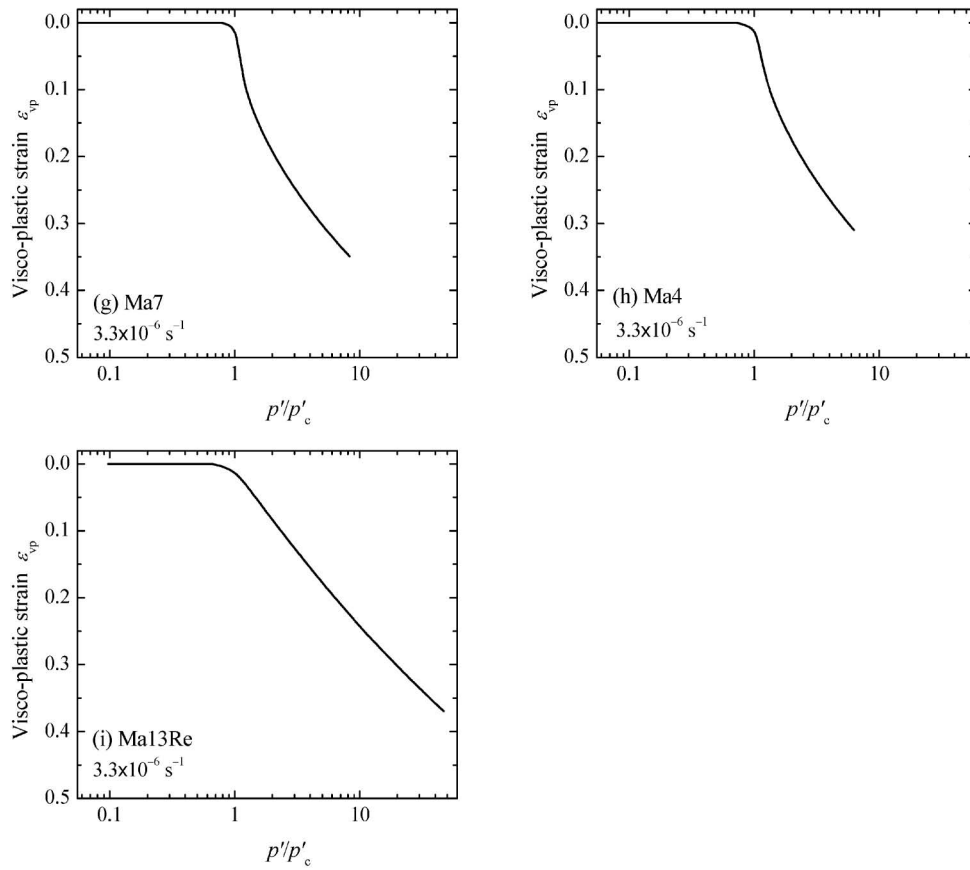


Fig. 5. (continuation)

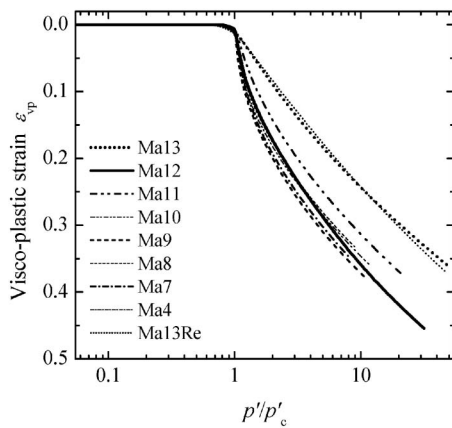


Fig. 6. Superimposed reference compression curves

is similar to the behavior in the overconsolidation range (described later) because the long-term p is not significantly greater than p'_c .

In the overconsolidation range in which the long-term p exists between σ'_{v0} and p'_c , the primary consolidation ends rapidly; then, the secondary consolidation appears continuously. Settlement is considerably less during the early secondary consolidation stage; however, the consolidation curve becomes convex shaped after approximately 1.0×10^3 min, thus indicating that the slope $\Delta \varepsilon_{vp} / \Delta \log t$ increases with the logarithmic time. The slope

$\Delta \varepsilon_{vp} / \Delta \log t$ is the coefficient of secondary consolidation in ε_{vp} , and hereafter it is denoted as $C_{\alpha \varepsilon_{vp}}$. The points corresponding to the $\dot{\varepsilon}_{vp}$ ($= \Delta \varepsilon_{vp} / \Delta t$) values of 3.3×10^{-5} (only some cases), 3.3×10^{-6} , 3.3×10^{-7} , 3.3×10^{-8} , and $3.3 \times 10^{-9} \text{ s}^{-1}$ are shown on the curves.

DISCUSSION OF TEST RESULTS WITH ISOTACHE CONCEPT

The consolidation yield stress corresponding to a $\dot{\varepsilon}_{vp}$ value of $3.3 \times 10^{-6} \text{ s}^{-1}$, which is equivalent to the basic test condition of the CRS tests, is denoted as p'_{c0} , as mentioned above. For Ma12, the CRS test was carried out for an $\dot{\varepsilon}$ value of $3.3 \times 10^{-8} \text{ s}^{-1}$; however, p'_{c0} corresponds to an $\dot{\varepsilon}$ value of $3.3 \times 10^{-6} \text{ s}^{-1}$.

The test results obtained from the CRS and LT tests are treated according to the flowchart shown in Fig. 8. The values of ε_{vp} corresponding to the $\dot{\varepsilon}_{vp}$ values of 3.3×10^{-5} , 3.3×10^{-6} , 3.3×10^{-7} , 3.3×10^{-8} , and $3.3 \times 10^{-9} \text{ s}^{-1}$ are obtained from the LT test results in the normal consolidation range ($p > 1.15 \times p'_{c0}$). Here, the data in the overconsolidation range were not used because some of the data were significantly variable, probably due to sample disturbance. The consolidation yield stress p'_c is obtained as a function of $\dot{\varepsilon}_{vp}$ from the reference compression curve by using the data set of p' and ε_{vp} . The fitting parameters c_1 , c_2 , and p'_{cL} (called as isotache parameters hereafter) in Eq. (8) are adjusted to the $\log p'_c$ - $\log \dot{\varepsilon}_{vp}$ relationship. The

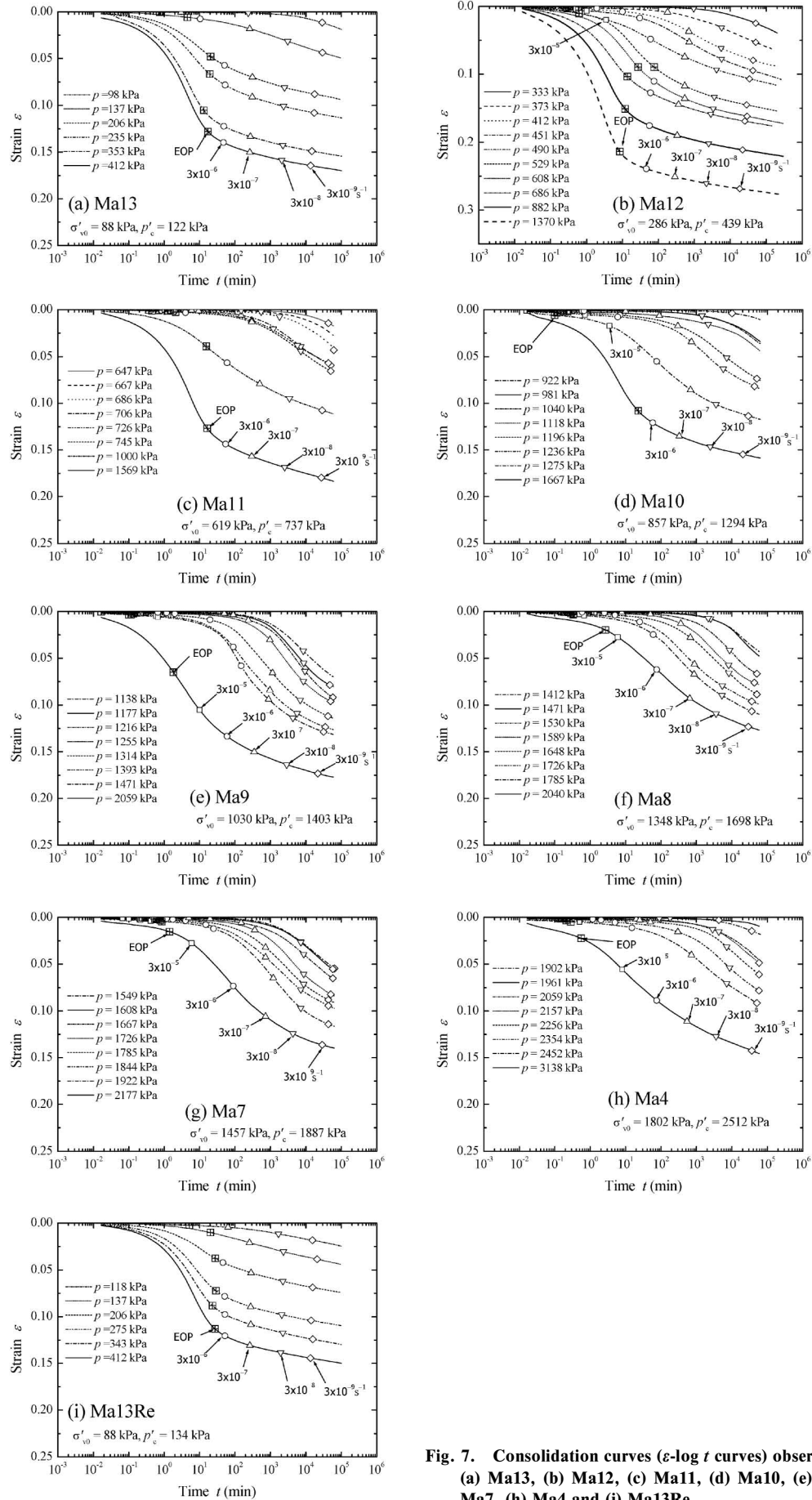


Fig. 7. Consolidation curves (ε -log t curves) observed in the LT tests: (a) Ma13, (b) Ma12, (c) Ma11, (d) Ma10, (e) Ma9, (f) Ma8, (g) Ma7, (h) Ma4 and (i) Ma13Re

fitting is performed by the least square method for c_1 and c_2 for various p'_{cL} values. Then, the best isotache parameters with the minimum error are determined. The vertical axis representing p'_c for the fitting curve is normalized by p'_{c0LT} . Here, p'_{c0LT} is defined as the p'_c corre-

sponding to an $\dot{\epsilon}_{vp}$ value of $3.3 \times 10^{-6} \text{ s}^{-1}$ on the fitting curve. The parameter p'_{c0} obtained from the CRS test is denoted as p'_{c0CRS} in order to distinguish it from p'_{c0LT} .

The $\log p'_c/p'_{c0LT} - \log \dot{\epsilon}_{vp}$ relationships evaluated with Eq. (8) are indicated by solid lines in Fig. 9. From the definition, the curves pass through $p'_c/p'_{c0LT} = 1$ at $\dot{\epsilon}_{vp} = 3.3 \times 10^{-6} \text{ s}^{-1}$. The dotted lines corresponding to $p'_c/p'_{c0LT} = 0.55$ will be discussed later. In Ma10 and Ma9, the $\epsilon_{vp} - \log p'_c$ relationships obtained from the CRS and LT tests with the isotache model, respectively, were not in agreement. This is probably due to some different properties of the specimens examined in the CRS and LT tests. In order to obtain good agreement between them, the reference compression curves were expanded (1.1 times) for Ma10 and contracted (0.8 times) for Ma9, along the ϵ_{vp} direction.

All the test results in the normal consolidation range for Ma13, Ma12, and Ma11 show a unique relationship. This fact indicates that there is a unique $\log p'_c/p'_{c0LT} - \log \dot{\epsilon}_{vp}$ relationship for each sample consolidated in the normal consolidation range. The fitting with Eq. (8) was successfully performed for each sample. This implies that Eq. (8) is widely applicable as an isotache model. The isotache parameters obtained by the fitting are listed in Table 3.

Because the range of $\dot{\epsilon}_{vp}$ was limited in the range from 10^{-9} to 10^{-5} s^{-1} , $\dot{\epsilon}_{vp}$ corresponding to p'_{cL} (i.e., $\dot{\epsilon}_{vp} = 0$) was very far from this range. Thus, it cannot be denied that the value of p'_{cL} determined above possessed lower relia-

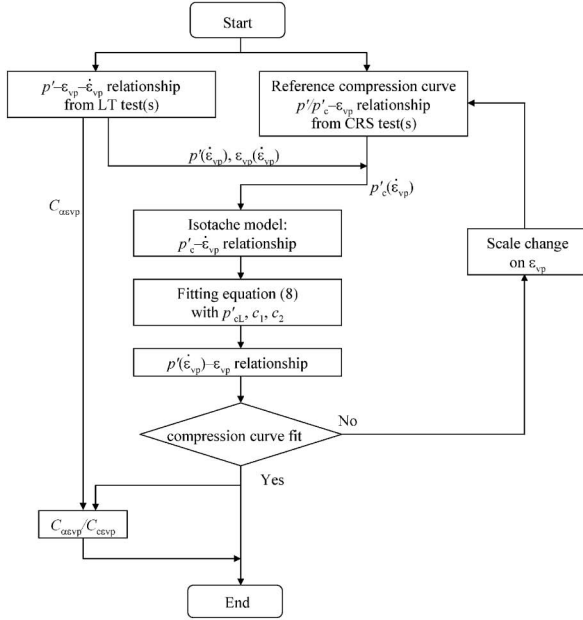


Fig. 8. Flowchart for the data treatment based on the isotache model

Table 3. The isotache parameters obtained by the fitting with Eq. (8)

Same	σ'_{v0} (kPa)	p'_{c0CRS} (kPa)	p'_{c0LT} (kPa)	p'_{cL} (kPa)	p'_{cL}/p'_{c0LT}	c_1	c_2
Ma13	88	122	133	67	0.504	1.128	0.0903
Ma12	286	439	448	280	0.625	1.228	0.1377
Ma11	619	737	813	372	0.458	1.196	0.0813
Ma10	857	1294	1211	862	0.712	0.617	0.1205
Ma9	1030	1403	1198	670	0.559	1.731	0.1561
Ma8	1348	1698	1736	922	0.531	1.097	0.0967
Ma7	1457	1887	1809	1121	0.620	1.093	0.1253
Ma4	1802	2512	2423	1091	0.450	1.192	0.0786
Ma13Re	(98)	134	151	99	0.656	1.209	0.1467

Table 4. The isotache parameters obtained by the fitting with Eq. (8) and $p'_{cL} = 0.55 \times p'_{c0LT}$

Same	σ'_{v0} (kPa)	p'_{c0CRS} (kPa)	p'_{c0LT} (kPa)	p'_{cL} (kPa)	p'_{cL}/p'_{c0LT}	c_1	c_2
Ma13	88	122	133	73	0.55	1.11	0.103
Ma12	286	439	447	246	0.55	1.09	0.103
Ma11	619	737	814	447	0.55	1.13	0.105
Ma8	1348	1698	1736	955	0.55	1.09	0.102
Ma7	1457	1887	1811	995	0.55	1.05	0.099
Ma4	1802	2512	2420	1333	0.55	1.07	0.101
Ma13Re	—	134	150	83	0.55	1.01	0.097

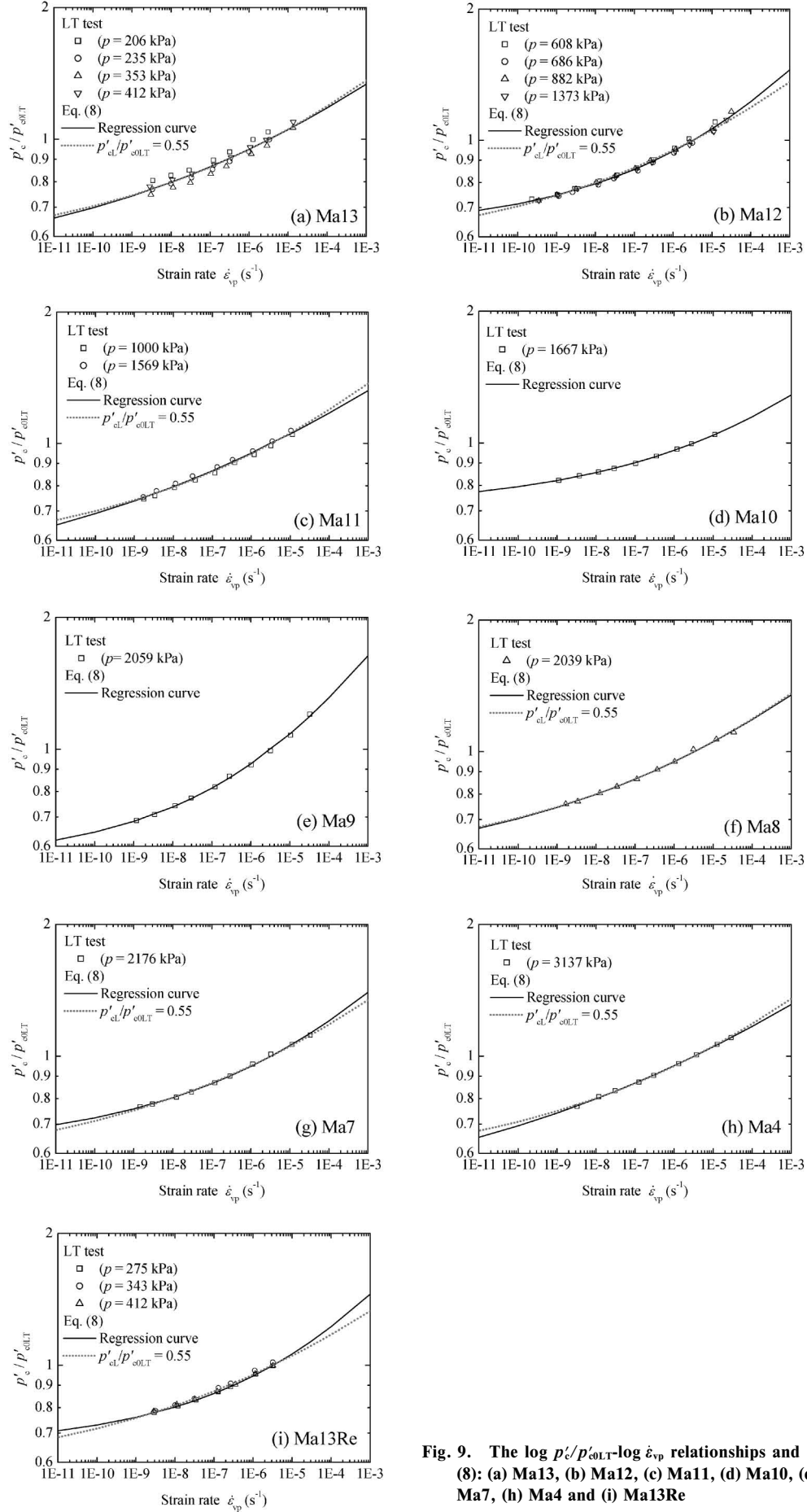


Fig. 9. The $\log p'_e/p'_{e,LT}$ - $\log \dot{\epsilon}_{vp}$ relationships and the fitting with Eq. (8): (a) Ma13, (b) Ma12, (c) Ma11, (d) Ma10, (e) Ma9, (f) Ma8, (g) Ma7, (h) Ma4 and (i) Ma13Re

bility. Ohmukai and Imai (2006) concluded that the lower limit of p'_c at $\dot{\epsilon}_{vp} = 1 \times 10^{-11} \text{ s}^{-1}$ was $0.71 \times p'_{c0}$ for the Osaka Bay clay retrieved from the Kansai International Airport. Thus, a common value of p'_{cL}/p'_{c0LT} can probably be determined for the clays. In fact, the p'_{cL}/p'_{c0LT} values for all the samples, including Ma13Re, are in the narrow range of 0.549 ± 0.084 (COV=0.15), except for Ma10 and Ma9 in which the reference compression curves were expanded or contracted for adjustment.

Consequently, we decide to use $p'_{cL}/p'_{c0LT} = 0.55$ as the common value for the clays examined in this study. By using this value, c_1 and c_2 are again determined by the least square method, except for Ma10 and Ma9. The isotache parameters are listed in Table 4. The regression curves are shown as dotted lines in Fig. 9. The fitting curves with a p'_{cL}/p'_{c0LT} value of 0.55 and the test results are compared thoroughly.

In Table 4, c_1 and c_2 are evaluated as 1.08 ± 0.04 (COV = 0.04) and 0.101 ± 0.003 (COV = 0.026). These small

COV values indicate that there are common values for these parameters among the Holocene clay, even its reconstituted form, and the Pleistocene clay. The microfabric of an undisturbed clay and that of its reconstituted form are significantly different, as shown by Watabe et al. (2007b). The reference curves of the Holocene clays (Ma13 and Ma13Re) were significantly different from those of the Pleistocene clays (Ma12 and deeper ones). However, it is very interesting that the isotache parameters in the normal consolidation range can be commonly determined for all the specimens of the Osaka Bay clay examined in this study.

Using Eq. (8) along with the isotache parameters (p'_{cL} , c_1 , and c_2) listed in Table 4 and those listed in Table 3 for Ma9 and Ma10, p'_c is determined as a function of $\dot{\epsilon}_{vp}$. The compression curve (ϵ_{vp} - $\log p'$ curve) corresponding to a given $\dot{\epsilon}_{vp}$ is obtained by multiplying p'/p'_c of the reference compression curve by $p'_c(\dot{\epsilon}_{vp})$. The compression curves derived from the test results by using the isotache model

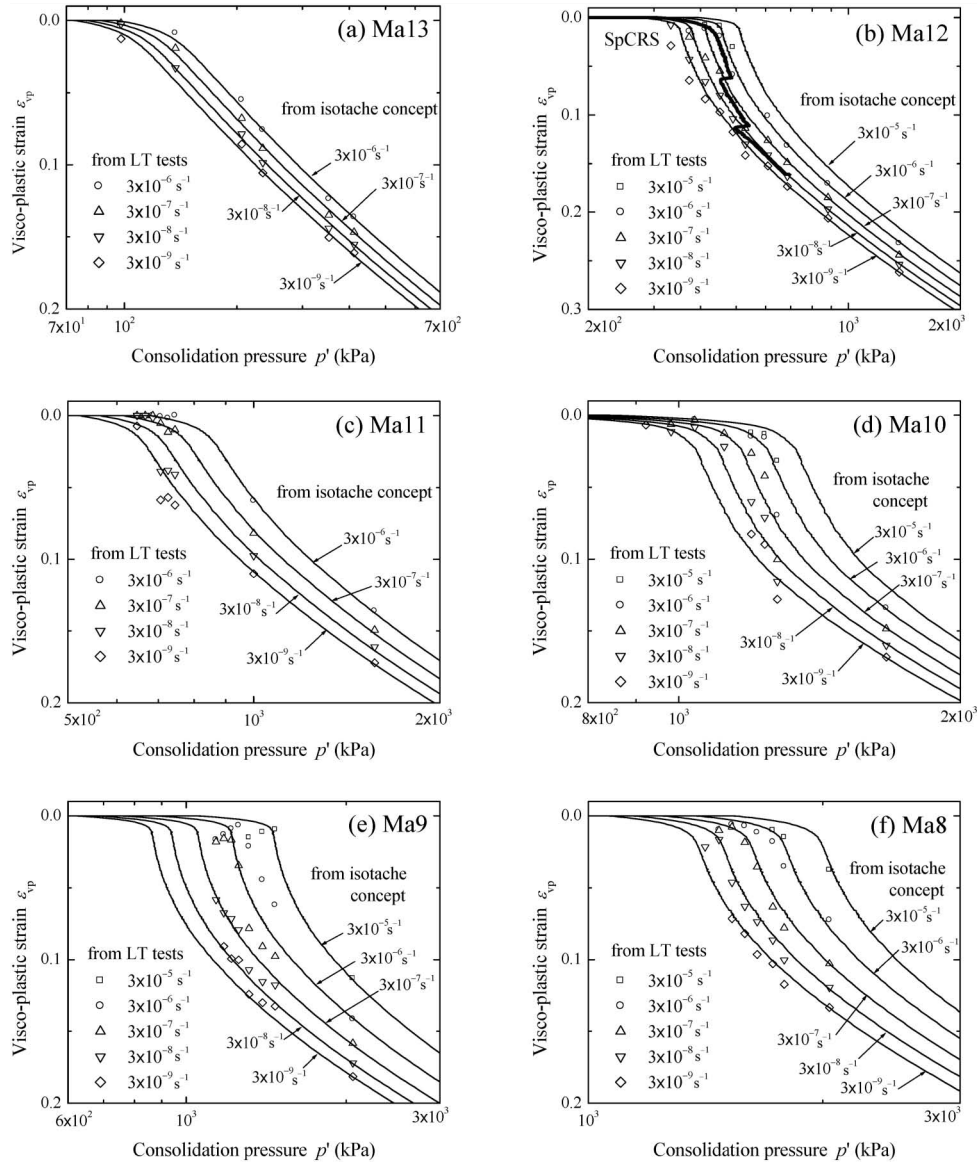


Fig. 10. Compression curves (ϵ_{vp} - p' curves): (a) Ma13, (b) Ma12, (c) Ma11, (d) Ma10, (e) Ma9, (f) Ma8, (g) Ma7, (h) Ma4 and (i) Ma13Re

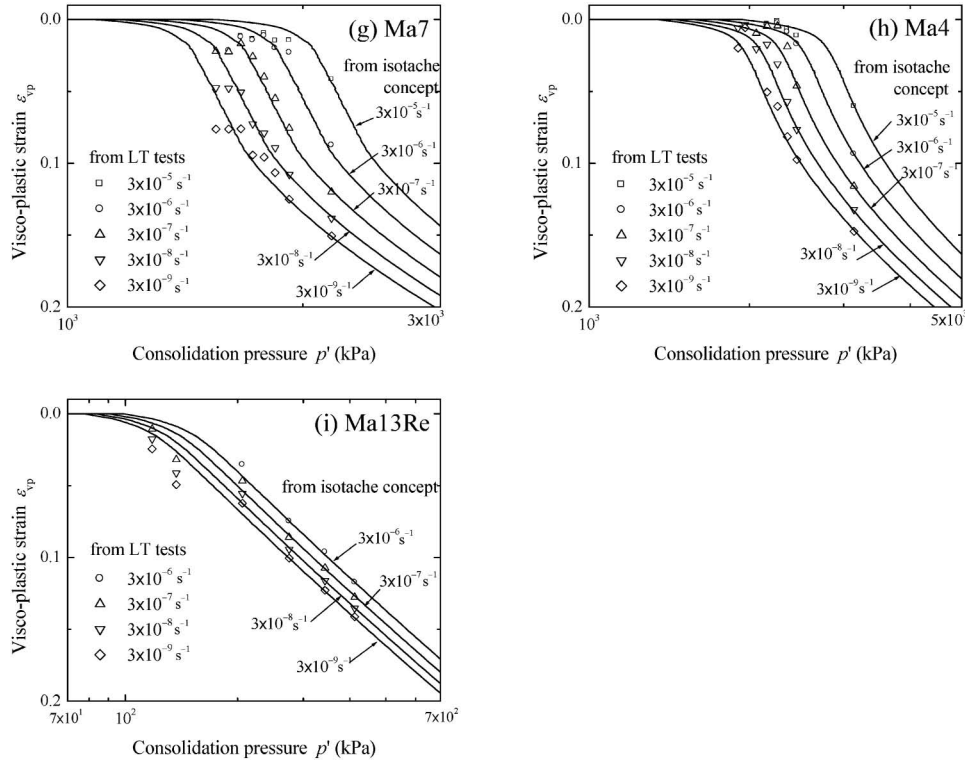


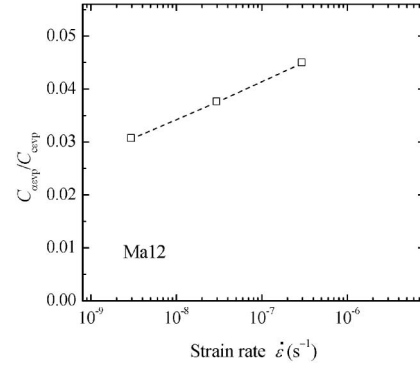
Fig. 10. (continuation)

corresponding to $\dot{\epsilon}_{vp} = 3.3 \times 10^{-5}$, 3.3×10^{-6} , 3.3×10^{-7} , 3.3×10^{-8} , and $3.3 \times 10^{-9} \text{ s}^{-1}$ are shown in Fig. 10. The (ϵ_{vp}, p') data, which is obtained from the secondary consolidation curves in the LT tests, are also plotted as a function of $\dot{\epsilon}_{vp}$ in this figure. The compression curves of the isotache model and the data from the LT test are compared thoroughly, even for Ma10 and Ma9. However, for Ma10 and Ma9, it must be noted that the isotache parameters in Eq. (8) are significantly different from the isotache parameters of the other curves; moreover, we used expanded and contracted reference compression curves.

In the above discussion, the isotache model was applied only to the data obtained in the normal consolidation range. However, it is very interesting to note that the modeling was successfully performed in not only the normal consolidation range but also the overconsolidation range by using the reference compression curve that included the overconsolidation section. Further, it should be noted that the isotache model is very practical because it uses only a reference compression curve and three isotache parameters (p'_{cL} , c_1 , and c_2) in Eq. (8).

For Ma12, a special CRS test (SpCRS test) was also carried out for three values of strain rate in different stages: first, $3.3 \times 10^{-6} \text{ s}^{-1}$; then, $3.3 \times 10^{-7} \text{ s}^{-1}$; and finally, $3.3 \times 10^{-8} \text{ s}^{-1}$. The compression curve observed in this test is also shown in Fig. 10(b). When the ϵ_{vp} - $\log p'$ curves derived from the LT test using the isotache model and that observed in the SpCRS test were compared thoroughly, it indicated that the isotache model is widely applicable to the LT test results.

The coefficient of secondary consolidation in the visco-

Fig. 11. $C_{\alpha vp}/C_{\epsilon vp}$ - $\dot{\epsilon}_{vp}$ relationship for Ma12

plastic strain, $C_{\alpha vp}$, at a certain instant is obtained from the consolidation curve of the LT test. The compression index in the visco-plastic strain, $C_{\epsilon vp}$, corresponding to both $\dot{\epsilon}_{vp}$ and ϵ_{vp} at that instant is obtained from the reference compression curve as $C_{\epsilon vp}(p'/p'_c) = \Delta \epsilon_{vp} / \Delta \log(p'/p'_c)$. The quantity $C_{\alpha vp}/C_{\epsilon vp}$ is then calculated as a function of $\dot{\epsilon}_{vp}$ for a given p' . As an example, the $C_{\alpha vp}/C_{\epsilon vp}$ - $\dot{\epsilon}_{vp}$ relationship for Ma12 is shown in Fig. 11. The quantity $C_{\alpha vp}/C_{\epsilon vp}$ tends to decrease with decreasing $\dot{\epsilon}_{vp}$. This phenomenon is inconsistent with the constant C_{α}/C_{ϵ} concept proposed by Mesri and Castro (1987). On the other hand, the $C_{\alpha vp}/C_{\epsilon vp}$ values corresponding to $\dot{\epsilon}_{vp} = 3.3 \times 10^{-8} \text{ s}^{-1}$ for the undisturbed samples, except for Ma10 and Ma9, are plotted as 0.039 ± 0.003 in a very narrow range in Fig. 12. This range is consistent with the range of 0.04 ± 0.01 proposed by Mesri and Castro (1987).

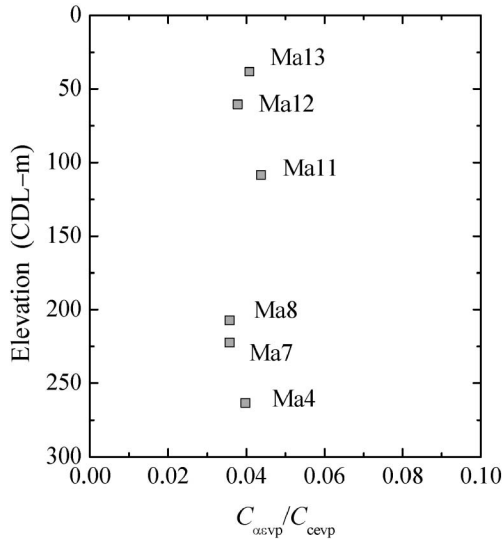


Fig. 12. Depth profile of $C_{\alpha vp}/C_{c vp}$ corresponding to an $\dot{\epsilon}_{vp}$ value of $3.3 \times 10^{-8} \text{ s}^{-1}$

In Eq. (8), $p'_c(\dot{\epsilon}_{vp})$ decreases with decreasing $\dot{\epsilon}_{vp}$; however, p'_c asymptotically approaches toward to the lower limit of p'_{cL} . The fittings with this equation were performed well for the test results, as discussed above. Leroueil (2006) theoretically inferred that the slope α of the $\log p'_c/p'_{c0LT}-\log \dot{\epsilon}_{vp}$ relationship is equivalent to the ratio $C_{\alpha vp}/C_{c vp}$. It can be observed from Fig. 9 that α decreases with $\dot{\epsilon}_{vp}$. This implies that the constant C_{α}/C_c concept proposed by Mesri and Castro (1987) is not applicable in the range of small $\dot{\epsilon}_{vp}$ ($< 10^{-8} \text{ s}^{-1}$). As indicated by Leroueil (2006), the constant C_{α}/C_c is a rough approximation valid in a range of large $\dot{\epsilon}_{vp}$ (from 10^{-8} to 10^{-5} s^{-1}). This is consistent with the statement on the constant p'_c for $\dot{\epsilon}_{vp}$ smaller than $1 \times 10^{-11} \text{ s}^{-1}$ in Ohmukai and Imai (2006). It is noteworthy that when p'_{cL} decreases to zero in Eq. (9), Eq. (6), i.e., the constant C_{α}/C_c concept, is consequently derived.

In this study, the isotache concept expressed by Eqs. (1) and (2) (Leroueil et al., 1985) was applied to the Osaka Bay clays retrieved from the Kansai International Airport. As a result, it was clarified that the long-term consolidation of the Osaka Bay clay can generally be explained by the isotache concept by using Eq. (8) along with the reference compression curve. Here, Eq. (8) represents the visco-plastic strain rate effect evaluated by the LT test, and the reference compression curve represents the inherent compressibility evaluated by the CRS test. Eq. (8) proposed in this study provides a one-on-one relationship between p'_c and $\dot{\epsilon}_{vp}$ without any applicability limit on the range of $\dot{\epsilon}_{vp}$. This is useful for the practical calculation of the long-term consolidation settlement.

CONCLUSIONS

In this study, a simplified model of the isotache concept using the reference compression curve (Eq. (4)) and the $p'_c-\dot{\epsilon}_{vp}$ relationship (Eq. (8)) obtained from both the

CRS and LT tests is performed. This model is very practical because the reference compression curve and the isotache parameters (p'_{cL} , c_1 , and c_2) can be evaluated from a minimum of one CRS test and one LT test. The LT test should be conducted for the normal consolidation range.

Because the slope of $\log p'_c/p'_{c0LT}-\log \dot{\epsilon}_{vp}$ ($\alpha = C_{\alpha vp}/C_{c vp}$) tends to decrease with $\dot{\epsilon}_{vp}$, it was confirmed that the constant C_{α}/C_c concept is approximately applicable only in the range of large values of $\dot{\epsilon}_{vp}$. However, it can be stated that the constant C_{α}/C_c concept is useful in practice because the values of α for a given $\dot{\epsilon}_{vp}$ for all the examined samples are in a narrow range. It must be noted that the consolidation settlement is probably overestimated by using the constant C_{α}/C_c concept because the in-situ strain rate is very small.

All the test results for the samples examined in this study can be excellently described by the proposed isotache model.

This study showed that Eq. (8) is widely applicable to the Osaka Bay clay. Among the three isotache parameters (p'_{cL} , c_1 , and c_2) in Eq. (8), p'_{cL} was evaluated to have a common value of $0.55 \times p'_{c0}$ for the clays examined, where p'_{c0} is defined as p'_c at an $\dot{\epsilon}_{vp}$ value of $3.3 \times 10^{-6} \text{ s}^{-1}$. The isotache parameters evaluated in this study are listed in Table 4. When $p'_{cL} = 0.55 \times p'_{c0}$ was used, the other parameters c_1 and c_2 were also evaluated in narrow ranges as 1.08 ± 0.04 and 0.101 ± 0.003 , respectively, by the least squares method. This implies that the isotache parameters p'_{cL} , c_1 , and c_2 can be commonly determined for the Osaka Bay clays retrieved from the Kansai International Airport.

We are planning to simulate the long term consolidation with the isotache model proposed in this study and we shall report the results in the near future.

ACKNOWLEDGEMENTS

The study presented in this paper was carried out as a part of the collaborative research between Port and Airport Research Institute (PARI) and Kansai International Airport Land Development Co., Ltd. (KALD). We would like to thank Dr. Masaki Kobayashi of Coastal Development Institute of Technology (CDIT) for his active discussions on this study.

NOTATION

- a_1, a_2 : constants for Eq. (6)
- b_1, b_2 : constants for Eq. (7)
- c_1, c_2 : constants for Eq. (8)
- c'_1, c'_2 : constants for Eq. (9)
- C_c : compression index
- C_{ce} : C_c in strain
- $C_{c vp}$: C_c in visco-plastic strain
- COV: coefficient of variation
- C_{α} : coefficient of secondary consolidation
- $C_{\alpha e}$: C_{α} in strain
- $C_{\alpha vp}$: C_{α} in visco-plastic strain

OCR: overconsolidation ratio
 p : consolidation pressure
 p' : effective consolidation pressure
 p'_c : effective consolidation yield stress
 p'_{c0} : p'_c at $\dot{\epsilon} = 3.3 \times 10^{-6} \text{ s}^{-1}$
 p'_{c0LT} : p'_{c0} obtained from LT test
 p'_{c0CRS} : p'_{c0} obtained from CRS test
 p'_{cL} : lower limit of p'_c
 t : elapsed time for consolidation
 α : slope of $\log p'_c/p'_{c0LT} - \log \dot{\epsilon}_{vp}$ ($= C_{\alpha evp}/C_{cev}$)
 ϵ : strain
 $\dot{\epsilon}$: strain rate ($= \Delta\epsilon/\Delta t$)
 ϵ_{v0} : strain at $p' = \sigma'_{v0}$
 ϵ_e : elastic strain
 ϵ_{vp} : visco-plastic strain
 Δu : excess pore water pressure
 σ'_{v0} : overburden effective stress

REFERENCES

- Adachi, T., Oka, F. and Mimura, M. (1996): Modeling aspects associated with time dependent behavior of soils, *Session on Measuring and Modeling Time Dependent Soil Behavior, ASCE Convention, Washington, Geot. Special Publication*, (61), 61–95.
- Akai, K. (2000): Insidious settlement of super-reclaimed offshore seabed, *Proc. Int. Symp. Coastal Geotech. Engrg. Practice, IS-Yokohama 2000*, 1, 243–248.
- Bjerrum, L. (1967): Engineering geology of normally consolidated marine clays as related to the settlement of buildings, *Géotechnique*, 17(2), 83–119.
- Duncan, J. M. (1993): Limitations of conventional analysis of consolidation settlement, *J. Geotech. Engrg.*, ASCE, 119(9), 1333–1359.
- Horie, H., Zen, K., Ishii, I. and Matsumoto, K. (1984): Engineering properties of marine clay in Osaka bay, (Part-1) Boring and sampling, *Technical Note of Port and Harbour Res. Inst.*, Ministry of Transport, Japan, (498), 5–45 (in Japanese).
- Imai, G., Ohmukai, N. and Tanaka, H. (2005): An isotaches-type compression model for predicting long term consolidation of KIA clays, *Proc. Symp. Geotech. Aspects of Kansai Int. Airport*, 49–64.
- Kanda, K., Suzuki, S. and Yamagata, N. (1991): Offshore soil investigation at the Kansai International Airport, *Proc. GEO-COAST '91*, 1, 33–38.
- Kim, Y. T. and Leroueil, S. (2001): Modelling the viscoplastic behaviour of clays during consolidation: application to Berthierville clay in both laboratory and field conditions, *Can. Geotech. J.*, 38(3), 484–497.
- Kobayashi, M., Furudoi, T., Suzuki, S. and Watabe, Y. (2005): Modeling of consolidation characteristics of clays for settlement prediction of Kansai International Airport, *Proc. Symp. Geotech. Aspects Kansai Int. Airport*, 65–76.
- Leroueil, S., Kabbaj, M., Tavenas, F. and Bouchard, R. (1985): Stress-strain-strain rate relation for the compressibility of sensitive natural clays, *Géotechnique*, 35(2), 159–180.
- Leroueil, S. (2006): The isotache approach. Where are we 50 years after its development by Professor Šuklje? (2006 Prof. Šuklje's Memorial Lecture), *13th Danube-European Conference on Geotechnical Engineering, Ljubljana 2006*, 55–88.
- Mesri, G. and Choi, Y. K. (1985): The uniqueness of the end-of-primary (EOP) void ratio-effective stress relationship, *Proc. 11th ICSMFE, San Francisco*, 2, 587–590.
- Mesri, G. and Castro, A. (1987): The C_{α}/C_{ϵ} concept and K_0 during secondary compression, *J. Geotech. Engrg.*, ASCE, 113(3), 230–247.
- Mimura, M. and Jang, W. J. (2005): Long-term settlement of the Pleistocene deposits due to construction of KIA, *Proc. Symp. Geotech. Aspects Kansai Int. Airport*, 77–86.
- Nakase, A. (1987): Kansai International Airport-Construction of Man-Made Island, *Proc. 8th Asian Reg. Conf. of SMFE, Kyoto*, 2, 87–101.
- Ohmukai, N. and Imai, G. (2006): Evaluation of the strain rate dependency on consolidation yield stress of natural clays, *JSCE J. Geotech. Geoenviron. Engrg.*, 62(3), 579–592 (in Japanese).
- Šuklje, L. (1957): The analysis of the consolidation process by the isotache method, *Proc. 4th ICSMFE.*, London, 1, 200–206.
- Tanaka, H. and Locat, J. (1999): A microstructural investigation of Osaka Bay clay: the impact of microfossils on its mechanical behaviour, *Can. Geotech. J.*, 36, 493–508.
- Tanaka, H., Tanaka, M., Suzuki, S. and Sakagami, T. (2003): Development of a new cone penetrometer and its application to great depths of Pleistocene clays, *Soils and Foundations*, 43(6), 51–61.
- Tanaka, H. (2005): Consolidation behavior of natural soils around p_c value –Long term consolidation test–, *Soils and Foundations*, 45(3), 83–95.
- Tanaka, H., Udaka, K. and Nosaka, T. (2006): Strain rate dependency of cohesive soils in consolidation settlement, *Soils and Foundations*, 46(3), 315–322.
- Watabe, Y. and Tsuchida, T. (2001): Influence of stress release on sample quality of Pleistocene clay collected from large depth in Osaka Bay, *Soils and Foundations*, 41(4), 17–24.
- Watabe, Y., Tsuchida, T. and Adachi, K. (2002): Undrained shear strength of Pleistocene clay in Osaka Bay, *J. Geotech. Geoenviron. Engrg.*, ASCE, 128(3), 216–226.
- Watabe, Y., Tanaka, M., Tanaka, H. and Tsuchida, T. (2003): K_0 -consolidation in a triaxial cell and evaluation of in-situ K_0 for marine clays with various characteristics, *Soils and Foundations*, 43(1), 1–20.
- Watabe, Y., Shiraishi, Y., Murakami, T. and Tanaka, M. (2007a): Variability of physical and consolidation test results for relatively uniform clay samples retrieved from Osaka Bay, *Soils and Foundations*, 47(4), 701–716.
- Watabe, Y., Ishii, H., Kang, M.-S. and Saitoh, K. (2007b): Influence of sedimentation process on microfabric of clay deposit, *Proc. 13th Asian Reg. Conf. of SMGE, Kolkata*, 97–100.
- Yin, J. H., Graham, J., Clark, J. L. and Gao, L. (1994): Modelling unanticipated pore-water pressures in soft clays, *Can. Geotech. J.*, 31, 773–778.
- Yoshikuni, H., Nishiumi, H., Ikegami, S. and Seto, K. (1994): The creep and effective-stress-relaxation behavior on one-dimensional consolidation, *Proc. 29th Japan National Conference on Soil Mech. Found. Engrg.*, 1, 269–270 (in Japanese).